



Dalton
Transactions

**Synthesis, structural studies, and redox chemistry of
bimetallic [Mn(CO)₃] and [Re(CO)₃] complexes**

Journal:	<i>Dalton Transactions</i>
Manuscript ID	DT-ART-10-2020-003666.R1
Article Type:	Paper
Date Submitted by the Author:	09-Jan-2021
Complete List of Authors:	Henke, Wade; University of Kansas Kerr, Tyler; University of Kansas Sheridan, Thomas; California Institute of Technology Henling, Lawrence; California Institute of Technology Takase, Michael; California Institute of Technology Day, Victor; University of Kansas Gray, Harry; California Institute of Technology Blakemore, James; University of Kansas

SCHOLARONE™
Manuscripts

Synthesis, structural studies, and redox chemistry of bimetallic $[\text{Mn}(\text{CO})_3]$ and $[\text{Re}(\text{CO})_3]$ complexes†

Received 00th January 20xx,
Accepted 00th January 20xx

Wade C. Henke,^a Tyler A. Kerr,^{a,†} Thomas R. Sheridan,^{b,‡} Lawrence M. Henling,^b Michael K. Takase,^b Victor W. Day,^a Harry B. Gray,^b and James D. Blakemore^{a,b*}

DOI: 10.1039/x0xx00000x

Manganese ($[\text{Mn}(\text{CO})_3]$) and rhenium tricarbonyl ($[\text{Re}(\text{CO})_3]$) complexes represent a workhorse family of compounds with applications in a variety of fields. Here, the coordination, structural, and electrochemical properties of a family of mono- and bimetallic $[\text{Mn}(\text{CO})_3]$ and $[\text{Re}(\text{CO})_3]$ complexes are explored. In particular, a novel heterobimetallic complex featuring both $[\text{Mn}(\text{CO})_3]$ and $[\text{Re}(\text{CO})_3]$ units supported by 2,2'-bipyrimidine (bpm) has been synthesized, structurally characterized, and compared to the analogous monomeric and homobimetallic complexes. To enable a comprehensive structural analysis for the series of complexes, we have carried out new single crystal X-ray diffraction studies of seven compounds: $\text{Re}(\text{CO})_3\text{Cl}(\text{bpm})$, *anti*- $[\{\text{Re}(\text{CO})_3\text{Cl}\}_2(\text{bpm})]$, $\text{Mn}(\text{CO})_3\text{Br}(\text{bpz})$ (bpz = 2,2'-bipyrazine), $\text{Mn}(\text{CO})_3\text{Br}(\text{bpm})$, *syn*- and *anti*- $[\{\text{Mn}(\text{CO})_3\text{Br}\}_2(\text{bpm})]$, and *syn*- $[\text{Mn}(\text{CO})_3\text{Br}(\text{bpm})\text{Re}(\text{CO})_3\text{Br}]$. Electrochemical studies reveal that the bimetallic complexes are reduced at much more positive potentials ($\Delta E \geq 380$ mV) compared to their monometallic analogues. This redox behavior is consistent with introduction of the second tricarbonyl unit which inductively withdraws electron density from the bridging, redox-active bpm ligand, resulting in more positive reduction potentials. $[\text{Re}(\text{CO})_3\text{Cl}]_2(\text{bpm})$ was reduced with cobaltocene; the electron paramagnetic resonance spectrum of the product exhibits an isotropic signal (near $g = 2$) characteristic of a ligand-centered bpm radical. Our findings highlight the facile synthesis as well as the structural characteristics and unique electrochemical behavior of this family of complexes.

1. Introduction

Tricarbonyl complexes of the Group 7 transition metals (manganese, technetium, and rhenium) represent a privileged class of complexes that show remarkable versatility in studies of energy science,^{1,2,3} therapeutics,^{4,5} and electrocatalysis.^{6,7} The facile syntheses and numerous spectroscopic handles presented by these compounds have enabled fundamental insights to be gained over the years into how their structures give rise to useful properties as photosensitizers, carbon monoxide releasing molecules (CORMs), and electrocatalysts. The synthetic chemistry for the tricarbonyl complexes, which was developed early by Wrighton,⁸ Meyer,⁹ and Miguel,¹⁰ has led to explosive growth in research on $[\text{Re}(\text{CO})_3]$ ^{11,12,13,14,15} and $[\text{Mn}(\text{CO})_3]$ ^{16,17,18,19,20} chemistry.

In particular, diimine ligands are often used to support these tricarbonyl complexes; these ligands are attractive because they are readily prepared, easily derivatized, and make stable chelate complexes. Notably, 2,2'-bipyridyl (bpy) and 4,4'-disubstituted-2,2'-bipyridyl (^Rbpy) ligands have been frequently used in this area; installation of electron-donating or electron-withdrawing groups on the bpy ligand can readily tune the chemical, photophysical, and redox properties of the resulting complexes.²¹ In one study, Kubiak and co-workers utilized a range of electron-donating and electron-withdrawing ^Rbpy ligands to generate a series of $[\text{Re}(\text{CO})_3]$ complexes that

revealed ligand influences on the production of carbon monoxide (CO) from carbon dioxide (CO₂).²² Bocarsly and co-workers carried out related work with the $[\text{Mn}(\text{CO})_3]$ unit; the electron-donating and electron-withdrawing ^Rbpy ligands were shown to modulate the electrocatalytic properties of these complexes in a similar fashion.²³ More recently, some of us have been exploring the related coordination chemistry of $[\text{Mn}(\text{CO})_3]$ complexes bearing 4,5-diazafluorene (daf) ligands.²⁴ In comparison to $\text{Mn}(\text{CO})_3\text{Br}(\text{bpy})$, $\text{Mn}(\text{CO})_3(\text{daf})\text{Br}$ displays an increased bite angle which moderates the σ -donating and π -accepting abilities of daf, resulting in a unique electrochemical profile. Use of daf thus represents a complementary method for tuning often accomplished via traditional inductive effects. Considered together, these cases provide an appealing snapshot of the influence that diimine-type ligands can have on the properties of Group 7 tricarbonyl complexes.

An alternative strategy for tuning the properties of metal complexes involves development of heteromultimetallic systems.^{25,26} In such structures, the influence of one metal upon a second can be leveraged to engender new properties that are inaccessible with a single metal center alone. To accomplish work in this area, ditopic ligands are needed which can bring two metals into close proximity.^{27,28,29,30} In part thanks to their stability, $[\text{Mn}(\text{CO})_3]$ and $[\text{Re}(\text{CO})_3]$ moieties can be brought into close proximity. Several approaches have been employed for this purpose, including tethering alkyl groups,³¹ metal organic frameworks (MOFs),³² and multidentate ligands.³³ In particular, the chelating ligand 2,2'-bipyrimidine (bpm) is attractive for this purpose, as it offers direct synthetic access to both monometallic and bimetallic complexes. Superficially, bpm and bpy are similar ligands; however, the additional N-atoms in the bpm framework result in modulated donor properties compared to bpy. Synthetically, bpm is perhaps best known for

^a Department of Chemistry, University of Kansas, 1567 Irving Hill Road, Lawrence, Kansas 66045, USA. E-mail: blakemore@ku.edu; Tel: +1 (785) 864-3019

^b Beckman Institute and Division of Chemistry and Chemical Engineering, California Institute of Technology, Pasadena, California 91125, USA.

*Electronic Supplementary Information (ESI) available: Spectroscopic (NMR, EAS, EPR), electrochemical, and crystallographic (XRD) data. CCDC 2005315, 2005316, 2005317, 2005318, 2005319, 2005320, 2005321. For ESI and crystallographic data in CIF or other electronic format please see DOI: 10.1039/x0xx00000x

effectively bridging Ru centers,^{34,35} but it has also been successfully deployed to bridge between $[\text{Re}(\text{CO})_3]$ motifs.^{36,37}

In the 1980s, Vogler and co-workers first prepared the monometallic complex $\text{Re}(\text{CO})_3\text{Cl}(\text{bpm})$ (**1**).³⁶ Taking advantage of the additional bis-chelate site contained within **1**, they also synthesized the homobimetallic complex $[\text{Re}(\text{CO})_3\text{Cl}]_2(\text{bpm})$.³⁶ This species was also explored by Juris and co-workers³⁸ as well as Kaim and Kohlman.³⁹ In their report, elemental analysis data and emission spectroscopic properties were described for the characterization of $[\text{Re}(\text{CO})_3\text{Cl}]_2(\text{bpm})$. However, considering the structure of $[\text{Re}(\text{CO})_3\text{Cl}]_2(\text{bpm})$, there are two possible isomers, a situation recognized early by the others working in this arena.^{38,39} A syn isomer is possible which orients the halide ligands in the same direction (**2-syn**), as well as an anti isomer that orients the halides in opposite directions (**2-anti**).^{40,41} Vogler and co-workers did not explicitly state whether they were working with isomerically pure complexes, but based on previous studies^{37,38,39,40} and our work here (*vide infra*), we conclude that they were indeed studying a mixture of the **2-syn** and **2-anti** isomers (see Chart 1). More recently, Bocarsly and co-workers²³ and Jain and co-workers⁴² showed that the related monometallic Mn complexes $\text{Mn}(\text{CO})_3\text{Br}(\text{bpz})$ (**3**) and $\text{Mn}(\text{CO})_3\text{Br}(\text{bpm})$ (**4**) can be prepared. In light of the considerable interest in $[\text{Mn}(\text{CO})_3]$ complexes as catalysts and photoactive compounds,^{7,21} we were surprised to see that bimetallic complexes containing $[\text{Mn}(\text{CO})_3]$ moieties bridged by the bpm ligand have not been reported. Furthermore, there have been no prior crystallographic studies of either mono- or bimetallic $[\text{Mn}(\text{CO})_3]$ bpm complexes, motivating structural work to complement findings available regarding the structures of $[\text{Re}(\text{CO})_3]$ complexes with bpm.^{40,43,44,45,46,47}

Here, we report the syntheses, solid-state structures, and electrochemical properties of a family of $[\text{Re}(\text{CO})_3]$ and $[\text{Mn}(\text{CO})_3]$ complexes, including compounds $[\text{Mn}(\text{CO})_3\text{Br}]_2(\text{bpm})$ (isolable as a mixture of **5-syn** and **5-anti**) and $[\text{Re}(\text{CO})_3\text{Br}(\text{bpm})\text{Mn}(\text{CO})_3\text{Br}]$ (also isolable as a mixture of **6-syn** + **6-anti**, see Chart 1). Consistent with prior work on homobimetallic Re compounds of bpm, both the syn and anti isomers of $[\text{Mn}(\text{CO})_3\text{Br}]_2(\text{bpm})$ and $[\text{Re}(\text{CO})_3\text{Br}(\text{bpm})\text{Mn}(\text{CO})_3\text{Br}]$ are accessible based on NMR spectroscopy; the isomers are confirmed here by crystallographic studies of **5-syn**, **5-anti**, and **6-syn**. New solid-state structures of **1**,³⁶ **2-anti**,³⁶ **3**,²³ and **4**⁴² have also been collected for comparison to these new bimetallic compounds. In agreement with prior findings on $[\text{Mn}(\text{CO})_3(\text{diimine})]$ complexes,^{21,48} all of the $[\text{Mn}(\text{CO})_3]$ -containing compounds reported here are acutely light-sensitive. We find that the homo- and hetero-bimetallic Mn complexes undergo reduction at more positive potentials compared to their monometallic counterparts. Related electron paramagnetic resonance (EPR) studies reveal that chemical reduction of $[\text{Re}(\text{CO})_3\text{Cl}]_2(\text{bpm})$, which displays similar electrochemical properties to our new Mn compounds, involves a first ligand-centered reduction.^{49,50} Taken together, our studies suggest that the presence of a second tricarbonyl unit leads to a strong inductive effect that shifts the ligand-centred reduction process to more positive potentials in the cases of all the bimetallic compounds.

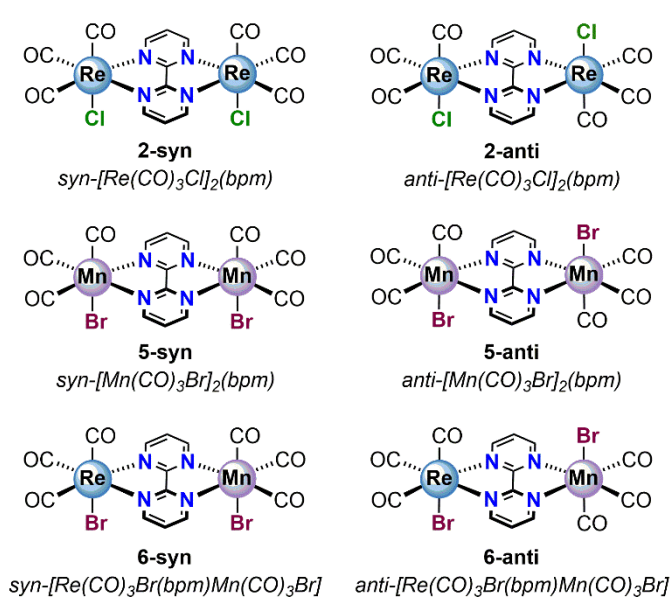
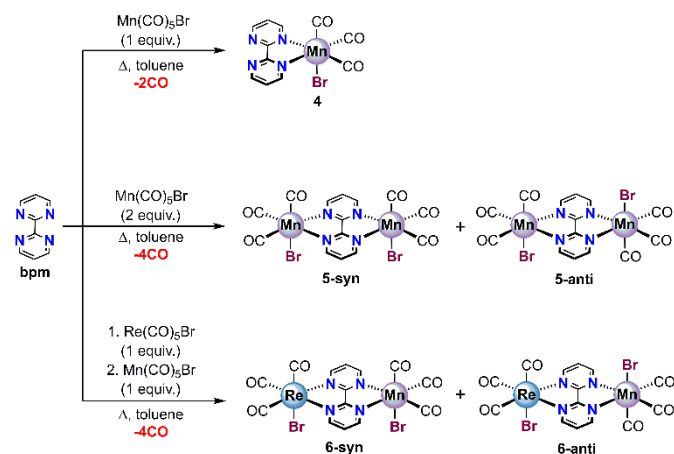


Chart 1: $[\text{Re}_2]$, $[\text{Mn}_2]$, and $[\text{ReMn}]$ bimetallic complexes described in this study. The dirhenium compounds were prepared according to Vogler and co-workers.³⁶

2. Results and Discussion

Synthesis and spectroscopic characterization

The synthons $\text{Re}(\text{CO})_5\text{Cl}$, $\text{Re}(\text{CO})_5\text{Br}$, and $\text{Mn}(\text{CO})_5\text{Br}$ were obtained from commercial suppliers, and monometallic **1**, **3**, and **4** were prepared according to the literature.^{23,36,42} Of particular interest to our group was the work carried out by Vogler and co-workers,³⁶ who reported the synthesis of the bimetallic complex, $[\text{Re}(\text{CO})_3\text{Cl}]_2(\text{bpm})$. Following their reported synthetic procedure, we isolated $[\text{Re}(\text{CO})_3\text{Cl}]_2(\text{bpm})$ as a mixture of **2-syn** and **2-anti** isomers; the appearance of the ^1H nuclear magnetic resonance (NMR) spectrum of the isolated material (see Figure S7) and the solid state structural data (see Figures S35-S36) confirm the presence of both the expected isomers.³⁷ Encouraged by these previous reports and keeping in mind that $[\text{Re}(\text{CO})_3\text{Cl}]_2(\text{bpm})$ can be isolated as a mixture of syn and anti isomers, our group pursued the synthesis of new homo- and heterobimetallic complexes bearing the $[\text{Mn}(\text{CO})_3]$ moiety using the bpm framework (see Scheme 1).



Scheme 1: Synthetic pathway for the generation of homo- and hetero-bimetallic complexes.

Due to the light sensitivity of these complexes, all reactions containing Mn were performed in the dark. In a refluxing suspension of toluene, $\text{Mn}(\text{CO})_5\text{Br}$ and bpm were combined in the appropriate stoichiometry (2 equiv. to 1 equiv., respectively) to generate $[\text{Mn}(\text{CO})_3\text{Br}]_2(\text{bpm})$, resulting in the formation of a mixture of the syn and anti isomers (**5-syn** and **5-anti**) in a good yield of 91%. The synthesis of the syn and anti isomers that are contained in the analogous $[\text{Re}(\text{CO})_3\text{Br}(\text{bpm})\text{Mn}(\text{CO})_3\text{Br}]$ (**6-syn** and **6-anti**) was accomplished by first generating the light-stable monometallic complex **1-Br** ($\text{Re}(\text{CO})_3\text{Br}(\text{bpm})$); $\text{Re}(\text{CO})_5\text{Br}$ was selected as the transition metal precursor to ensure that there would be no halide scrambling in solution upon formation of the bimetallic complex. Following the generation of **1-Br**, 1 equiv. of $\text{Mn}(\text{CO})_5\text{Br}$ was added to the solution to generate $[\text{Re}(\text{CO})_3\text{Br}(\text{bpm})\text{Mn}(\text{CO})_3\text{Br}]$, also as a mixture of **6-syn** and **6-anti** isomers in a good yield of 89%. Following successful generation of the mixtures of the desired complexes, they were each fully characterized (see Experimental Section and Supporting Information). Separation of the isomers of these new compounds was not pursued, although it may be possible based on our crystallographic studies (*vide infra*).

To begin characterization of the newly synthesized bimetallic complexes, we turned to ^1H NMR spectroscopy (see Figures S1–S7). In solution, complexes $[\text{Mn}(\text{CO})_3\text{Br}]_2(\text{bpm})$ and $[\text{Re}(\text{CO})_3\text{Br}(\text{bpm})\text{Mn}(\text{CO})_3\text{Br}]$ exist as a mixture of isomers with resonance splitting patterns arising from the $^3J_{\text{H,H}}$ and $^4J_{\text{H,H}}$ coupling in the aromatic region of their ^1H -NMR spectra. These signals correspond to the hydrogen atoms on the bpm ligands coordinated to their corresponding Mn and Re centers. The isomers **5-syn**, **5-anti**, **6-syn** and **6-anti** exhibit C_{2v} , C_{2h} , C_s , and C_s symmetry in solution, respectively, and this results in resonances that clearly distinguish the isomers of the homobimetallics **5-syn** and **5-anti** from the heterobimetallics **6-syn** and **6-anti**. The ^1H -NMR spectrum of the mixture containing **5-syn** and **5-anti** exhibits four unique protons in total which confirms that both the isomers are present. The different isomers of $[\text{Mn}(\text{CO})_3\text{Br}]_2(\text{bpm})$ are discernible from one another based on their different signal intensities; each isomer has a

corresponding triplet at δ 7.85 or 7.88 ppm (integrating to 2H) and doublet at δ 9.43 or 9.46 ppm (integrating to 4H) in the aromatic region. The isomers of $[\text{Mn}(\text{CO})_3\text{Br}]_2(\text{bpm})$ are present in an approximately 3:1 ratio based on the relative integration of the separated resonances at δ 9.43 and 9.46 ppm. Identifying which pair of resonances belongs to the **5-syn** or **5-anti** isomers based on the ^1H -NMR spectrum alone was not pursued here. Nonetheless, the expected connectivity of both isomers in solution is confirmed.

Considering the change in symmetry from C_{2v} and C_{2h} for **5-syn** and **5-anti** to C_s symmetry for **6-syn** or **6-anti**, we observed a significant change in the number of unique protons in the aromatic region of the ^1H -NMR spectrum. The decrease in the symmetry for **6-syn** and **6-anti** of $[\text{Re}(\text{CO})_3\text{Br}(\text{bpm})\text{Mn}(\text{CO})_3\text{Br}]$ in comparison to the **5-syn** and **5-anti** isomers of $[\text{Mn}(\text{CO})_3\text{Br}]_2(\text{bpm})$ results in a ^1H -NMR spectrum with peak groupings at 9.52, 9.27, and 7.86 ppm (integrating to 2H, 2H, 2H, respectively). Additionally, there is another resolved isomer with peak groupings at 9.55, 9.30, and 7.89 ppm (integrating to 2H, 2H, 2H). The isomers are present in an approximately 2:1 ratio based on the integration of the separated resonances at δ 9.52 and 9.55 ppm. ^1H -NMR alone did not identify which set of resonances belongs to **6-syn** or **6-anti**, but did confirm the expected connectivity in solution.

The bimetallic complexes $[\text{Mn}(\text{CO})_3\text{Br}]_2(\text{bpm})$ and $[\text{Re}(\text{CO})_3\text{Br}(\text{bpm})\text{Mn}(\text{CO})_3\text{Br}]$ have carbonyl ligands and are vividly colored in solution and thus we next turned to investigate their vibrational and absorption characteristics using infrared (IR) and electronic absorption (EA) spectroscopy (see Figure 1, and Figures S9 and S10–S13). The IR spectrum of **5-syn** and **5-anti** exhibits CO vibrational bands at 2031, 1952, and 1936 cm^{-1} , while the spectrum for **6-syn** and **6-anti** displays bands at 2028, 1951, 1935, and 1914 cm^{-1} . The observation of the additional band in the analysis of **6-syn** and **6-anti** compared to **5-syn** and **5-anti** is consistent with the decrease in symmetry for the heterobimetallic compounds (C_{2v} and C_{2h} for **5-syn** and **5-anti** to C_s for **6-syn** and **6-anti**).

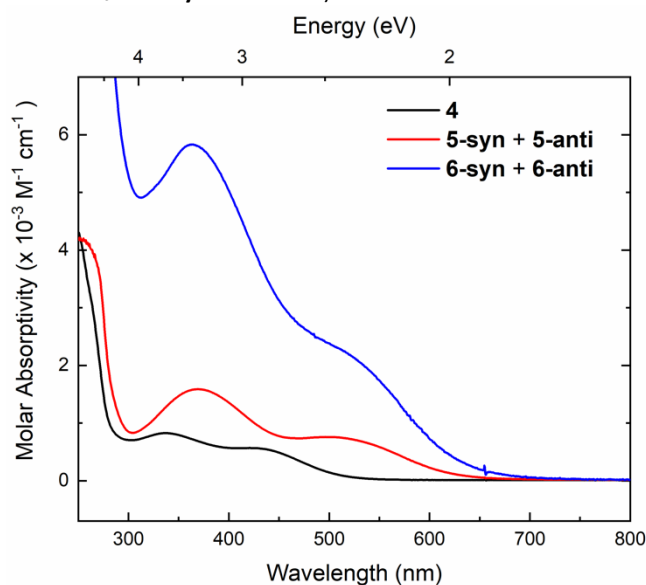


Figure 1: Electronic absorption spectra for **4**, **5-syn + 5-anti**, and **6-syn + 6-anti** in MeCN solution.

The EA spectrum of the mixture of **5-syn** and **5-anti** isomers of $[\text{Mn}(\text{CO})_3\text{Br}]_2(\text{bpm})$ exhibits two transitions in the visible region at 369 nm and 510 nm with molar absorptivities of $1600 \text{ M}^{-1} \text{ cm}^{-1}$ and $800 \text{ M}^{-1} \text{ cm}^{-1}$, respectively. The values of the molar absorptivities and the similarity of the spectrum to those of $\text{Mn}(\text{CO})_3\text{Br}(\text{bpy})$ and **4** (337 nm, $800 \text{ M}^{-1} \text{ cm}^{-1}$; 430 nm, $600 \text{ M}^{-1} \text{ cm}^{-1}$) enables their assignment as metal-to-ligand charge transfer (MLCT) transitions.⁵¹ Notably, the molar absorptivities associated with the charge transfer transitions in the syn and anti isomers of $[\text{Mn}(\text{CO})_3\text{Br}]_2(\text{bpm})$ are greater than those observed for the analogous monometallic **4**, which confirmed that the presence of the additional $[\text{Mn}(\text{CO})_3]$ unit plays a role in the light absorption properties of these complexes. We also investigated the EA properties of the mixture of **6-syn** and **6-anti** in the heterobimetallic compound $[\text{Re}(\text{CO})_3\text{Br}(\text{bpm})\text{Mn}(\text{CO})_3\text{Br}]$; the spectrum displays a similar absorption profile to **4** and the isomers of $[\text{Mn}(\text{CO})_3\text{Br}]_2(\text{bpm})$, with features at 364 nm ($5800 \text{ M}^{-1} \text{ cm}^{-1}$) and 515 nm ($2300 \text{ M}^{-1} \text{ cm}^{-1}$). The molar absorptivities of the electronic transitions associated with the syn and anti isomers of $[\text{Re}(\text{CO})_3\text{Br}(\text{bpm})\text{Mn}(\text{CO})_3\text{Br}]$ are three times greater than the comparable peaks in $[\text{Mn}(\text{CO})_3\text{Br}]_2(\text{bpm})$, and seven times greater than those associated with the monometallic complex **4**. These results suggest that the presence of a second tricarbonyl moiety increases the EA intensity, and suggest a distinct role for the heavier metal rhenium in engendering efficient light absorption.⁵²

X-ray diffraction studies

The syntheses of the monometallics **1**, **3**, and **4**, and the bimetallic complex $[\text{Re}(\text{CO})_3\text{Cl}]_2(\text{bpm})$ (**2-syn** and **2-anti**) have been previously described, but their solid-state structures have

not been reported to the Cambridge Structural Database (CSD).⁵³ To gain further insight into the properties of both the newly prepared and previously reported complexes, we turned to single crystal X-ray diffraction (XRD) analysis and report here seven new solid-state structures (see Figures 2 and S33-S43). The results confirm the expected *fac*-geometry of **1**, **3** and **4** with two equatorial CO ligands, an axial CO ligand, an axial halide, and the associated κ^2 -diimine ligand surrounding the rhenium or manganese center in each case. Based on the previous NMR analyses of $[\text{Re}(\text{CO})_3\text{Cl}]_2(\text{bpm})$, $[\text{Mn}(\text{CO})_3\text{Br}]_2(\text{bpm})$, and $[\text{Re}(\text{CO})_3\text{Br}(\text{bpm})\text{Mn}(\text{CO})_3\text{Br}]$, we anticipated that either or both of the syn and anti isomers could in principle be present in the solid-state. The results here confirm the presence of **2-syn**, **2-anti**, **5-syn**, **5-anti**, and **6-syn** in our solid-state samples; the syn isomers feature halides oriented in the same direction, and the anti isomers feature halides oriented in opposite directions. The structure for **2-anti**, in particular, reveals packing disorder (apparent in the axial chloride and CO ligands) driven by the presence of both **2-anti** and **2-syn** in the crystal unit cell; **2-anti** and **2-syn** are present in an 80:20 ratio. As **2-anti** predominates in the structure, we will refer to the structure here as being associated with the **2-anti** isomer. On the other hand, the packing disorder encountered for **2-anti** was not present in the data for **5-syn**, **5-anti**, or **6-syn** (see Figures S39-S43). Indeed, we were pleased to find that the individual crystals of **5-syn** and **5-anti** were visually distinguishable from one another in the vial; careful crystal harvesting ultimately led to their separate and unique solid-state structures. In the case of the heterobimetallic complex, only crystals of **6-syn** could be obtained.

The structures of the monometallic complexes **1**, **3**, and **4** closely resemble the well-known bpy-based complexes $\text{Re}(\text{CO})_3\text{X}(\text{bpy})$ (X = Cl, Br) and $\text{Mn}(\text{CO})_3\text{Br}(\text{bpy})$.^{54,55,56} A

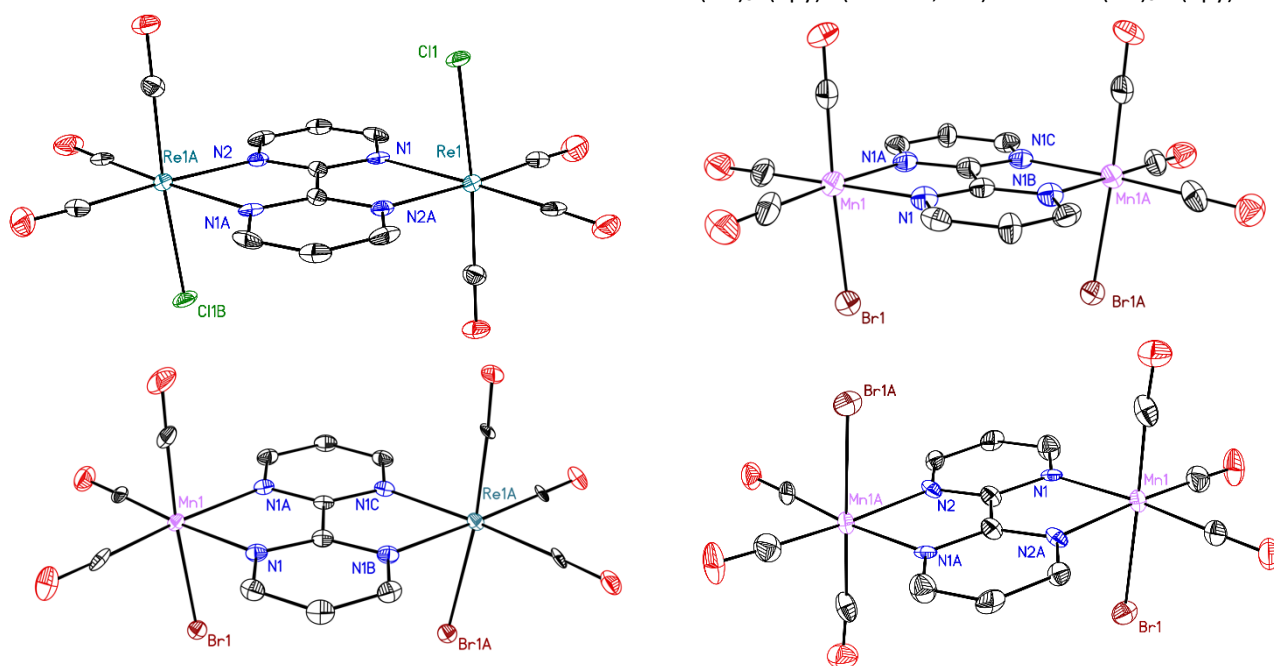


Figure 2: Solid-state structures of **2-anti** (upper-left), **5-syn** (upper-right), **5-anti** (lower-right), **6-syn** (lower-left). Displacement ellipsoids are shown at 50% probability level. Hydrogens and co-crystallized solvents are omitted for clarity.

Table 1: Selected bond lengths and distances in complexes **1**, **2-anti**, **3**, **4**, **5-syn**, **5-anti**, and **6-syn**.

Compound	Re-CO _{AX} (Å)	Re-CO _{EQ} (Å)	Re-N (Å)	Re-Halide (Å)	Mn-CO _{AX} (Å)	Mn-CO _{EQ} (Å)	Mn-N (Å)	Mn-Halide (Å)	BPM _{C-C} (Å)
1	1.894(6)	1.920(3), 1.926(3)	2.171(2), 2.172(3)	2.4837(10), 2.31(3)	-----	-----	-----	-----	1.484(4)
2-anti	1.894(15), 1.96(4)	1.934(7), 1.911(7)	2.192(5), 2.189(5)	2.455(3), 2.434(15)	-----	-----	-----	-----	1.456(12)
3	-----	-----	-----	-----	1.8132(14)	1.8253(14), 1.8272(14)	2.0277(11), 2.0379(11)	2.5255(2)	1.4602(18)
4	-----	-----	-----	-----	1.8257(17)	1.8115(16), 1.8197(15)	2.0450(12), 2.0478(12)	2.5332(3)	1.481(2)
5-syn	-----	-----	-----	-----	1.805(14)	1.806(9), 1.806(9)	2.062(6), 2.062(6)	2.521(2)	1.46(2)
5-anti	-----	-----	-----	-----	1.843(10)	1.812(10), 1.818(11)	2.061(7), 2.061(7)	2.5025(17)	1.435(17)
6-syn	1.933(14)	1.921(12), 1.921(12)	2.161(3), 2.161(3)	2.614(2)	1.825(16)	1.818(15), 1.818(15)	2.092(8), 2.092(8)	2.497(9)	1.451(7)

comparison of relevant bond lengths and angles of the monometallic Re complex **1** from this study with the structurally analogous complexes Re(CO)₃X(bpy) (X = **Cl**, **Br**) revealed very similar average Re–N distances of 2.172(4) Å (**1**), 2.175(7) Å (**Cl**), and 2.166(16) Å (**Br**) with N–Re–N bite angles of 74.85(9)° (**1**), 74.9(2)° (**Cl**), and 74.7(4)° (**Br**), respectively. Comparing the monometallic Mn-based complex **4** with the structurally similar complex Mn(CO)Br(bpy) revealed average Mn–N distances of 2.046(2) and 2.043(6) Å, and N–Mn–N bite angles of 79.5(3)° and 78.9(15)°, respectively. For both Re and Mn, we thus found that the presence of the additional nitrogen atoms on the bpm ligand does not induce significant structural changes in comparison to the complexes ligated with bpy. However, the bpm ligand has the attractive ability to chelate an additional tricarbonyl moiety to generate homo- and hetero-bimetallic complexes (see Table 1 and Figure 2).

Comparison of **1** with the homobimetallic **2-anti** revealed similar Re–CO_{AX} and Re–CO_{EQ} bond distances between the two complexes. A similar evaluation of the Mn-based monometallic complex **4** with the bimetallic complexes **5-syn** and **5-anti** showed that the Mn–CO_{AX} and Mn–CO_{EQ} bond distances remain indistinguishable within error as well. Thus, although the introduction of a second tricarbonyl moiety has a large effect on the electronics of the bimetallic complexes, this does not appear to correlate to significant structural changes when comparing the [M(CO)₃] units within **1**, **2-anti**, **4**, **5-syn** and **5-anti**.

Table 2: Selected bond angles in complexes **1**, **2-anti**, **3**, **4**, **5-syn**, **5-anti**, and **6-syn**.

Compound	N ₁ -Re-N ₂	N ₁ -Mn-N ₂
1	74.85(9)°	-----
2-anti	75.15(19)°	-----
3	-----	79.04(4)°
4	-----	78.68(5)°
5-syn	-----	79.5(3)°
5-anti	-----	79.7(3)°
6-syn	75.94(14)°	78.9(4)°

anti. On the other hand, there is a slight contraction in the metal-halide distances between the monometallic and homobimetallic complexes bearing the same transition metals, suggesting modulation of the donor power of the bpm ligand upon coordination of a second tricarbonyl unit. Furthermore, there are changes associated with the M–N bond distances, N–M–N bond angles, and d_{C-C} bond distances (d_{C-C} refers to the distance between the two central carbons connecting the individual pyrimidine rings) that result from the introduction of the second tricarbonyl unit.

In accord with these findings, comparison of **1** with **2-anti**, and **4** with **5-syn** and **5-anti** revealed elongation of the M–N bond lengths upon introduction of the second tricarbonyl unit. This likely occurs because initial introduction of a transition metal causes the bpm bite angle to narrow in an effort to facilitate metal binding. However, when a second metal tricarbonyl unit is introduced into the open site of a monometallic bpm complex, the nitrogen atoms are pulled back so that the optimal bite angle for both metal centers is established. Consistent with this proposal, we see a small increase in the bite angle upon generation of the homobimetallic complexes (see Table 2).

Further examination of the bond lengths around the bpm ligand for our series of complexes revealed a trend in the d_{C-C} bond distances; a slight contraction was observed when comparing the monometallic complexes to the bimetallic complexes. The solid-state structure of free bpm showed that the d_{C-C} bond length is 1.497(4) Å.⁵⁷ When we introduce Re or Mn to form a monometallic complex, we observed a small initial contraction of d_{C-C}, which is exacerbated further with the addition of a second metal to form the bimetallic complexes. This indicates that there is active backdonation from the transition metal to bpm and suggests that backbonding is further increased when a second metal is present. This trend was exciting to see since the C–C bond that binds the two pyridyl rings of bpy has also been observed to contract when

[Cp*Rh(bpy)Cl]PF₆ is reduced to Cp*Rh(bpy).^{58,59} Thus, some degree of backdonation from the electron-rich Re(I) and Mn(I) metal centers into the π^* orbitals of bpm may be present in these systems.

Overall, there are similar trends in the metrical parameters for both the manganese- and rhenium-containing species characterized here. This speaks to the modularity of the [M(CO)₃] units (M = Mn, Re) as judged by this structural work on the bpm framework. The inductive presence of an additional metal tricarbonyl unit, although giving rise to subtle changes to the solid-state structures, provides more pronounced effects on the electronic structure, as assessed by the EA spectroscopy. Consequently, we turned to cyclic voltammetry to identify further features that could distinguish the monometallic and bimetallic complexes.

Electrochemistry

The electrochemical properties of **1**, **3** and **4** have been previously described and were reconfirmed here for comparison to results on our new compounds (see Figures S17-S31).^{23,49} Cyclic voltammetry (CV) experiments using the monometallic complexes **1** and **4** were conducted with specific interest in determining the impact the additional nitrogen atoms on the bpm ligand could have on their electrochemical behavior with respect to the well-known analogues, Re(CO)₃Cl(bpy)^{6,22} and Mn(CO)₃Br(bpy).^{7,24} Based on prior studies, the electrochemical profile of Re(CO)₃Cl(bpy) exhibited an initial quasi-reversible ligand-centered reduction at -1.78 V followed by an irreversible metal-centered reduction at -2.16 V (all potentials are quoted versus ferrocenium/ferrocene, denoted Fc^{+/0}).²² As expected, the CVs of **1** are strikingly similar to Re(CO)₃Cl(bpy); an initial quasi-reversible reduction centered at -1.42 V was followed by an irreversible reduction at -1.91 V. These results indicate that Re(CO)₃Cl(bpy) and **1** behave in a similar fashion.

Mn(CO)₃Br(bpy) and **4** exhibit comparable CVs. Based on previous reports regarding Mn(CO)₃Br(bpy), the CV of this compound exhibits two irreversible reductions at -1.61 V and -1.83 V, coupled with an oxidation at -0.61 V.^{7,24} The presence of two irreversible reductions, while a more challenging case, can be readily explained and is consistent with a previously proposed mechanism.^{7,60} For the purpose of subsequent comparisons, the first irreversible wave can be attributed to a Mn-centred reduction that results in a 19e⁻ complex that loses the bound halide ligand, generating a transient 17e⁻ complex that dimerizes to form the 18e⁻ complex, [Mn(CO)₃(bpy)]₂. [Mn(CO)₃(bpy)]₂ can then be reduced at the more negative potential, a process that results in cleavage of the dimer to generate the formally 18e⁻ complex [Mn(CO)₃(bpy)]⁻. Scanning anodically, the oxidation of [Mn(CO)₃(bpy)]₂ can also be observed at a more positive potential. **4** thus behaves similarly to Mn(CO)₃Br(bpy), showing two irreversible reductions at -1.37 V and -1.58 V, and two irreversible oxidations at -1.36 V and -0.42 V. Notably, in comparison to Mn(CO)₃Br(bpy), complex **4** shows an additional oxidative feature at -1.36 V, suggesting that the electron-withdrawing ability of the additional nitrogen atoms present on bpm stabilizes one of the

reduced forms. Nonetheless, these findings suggest that the presence of the additional nitrogen atoms on bpm do not significantly impact the electrochemical profile, in terms of the number of the observable reduction events. However, the presence of the nitrogen atoms on the bpm ligand results in a noticeable inductive effect that shifts the reduction potentials of complexes **1** and **4** by *ca.* 250 mV in comparison to their corresponding bpy-based complexes.

With these results in hand, we investigated the cyclic voltammetry of the synthesized homo- and hetero-bimetallic complexes (see Figure 3). In each instance, [Re(CO)₃Cl]₂(bpm), [Mn(CO)₃Br]₂(bpm), and [Re(CO)₃Br(bpm)Mn(CO)₃Br] were interrogated as the mixture of their corresponding syn and anti isomers. These bimetallic compounds exhibit distinct electrochemical profiles in comparison to their monometallic analogues **1** and **4** (see Figure S24). In particular, the initial reduction for each of the bimetallic systems is quasi-reversible and at much more positive potentials than their comparable monometallic complexes (see Figure 3). The observation of an initial, quasi-reversible reduction is common for monometallic [Re(CO)₃]-based diimine systems, but is not observed for most [Mn(CO)₃]-based diimine systems. This suggests that the presence of an additional tricarbonyl moiety results in an inductive effect that shifts the initial reduction to much more positive potentials, significantly moderating the potential needed to introduce an electron into these systems. As a result, the first reduction for the isomers of [Re(CO)₃Cl]₂(bpm) is shifted by +600 mV and the first reduction for the isomers of [Mn(CO)₃Br]₂(bpm) is shifted by +380 mV in comparison to **1** and **4**, respectively. Intriguingly, the first reduction of the mixture of syn and anti isomers of [Re(CO)₃Br(bpm)Mn(CO)₃Br] falls in between the two homo-bimetallic complexes, further signifying that the electronic characteristics of this system are averaged between the two homobimetallics.

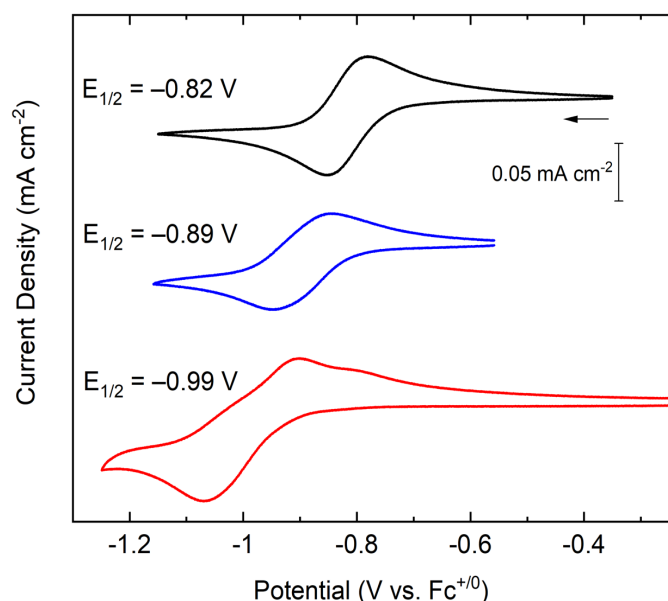


Figure 1: Cyclic voltammetry of $[\text{Re}(\text{CO})_3\text{Cl}]_2(\text{bpm})$ (**2-syn** and **2-anti**, black), $[\text{Re}(\text{CO})_3\text{Br}(\text{bpm})\text{Mn}(\text{CO})_3\text{Br}]$ (**6-syn** and **6-anti**, blue), and $[\text{Mn}(\text{CO})_3\text{Br}]_2(\text{bpm})$ (**5-syn** and **5-anti**, red), in MeCN solution with 0.1 M TBAPF₆ supporting electrolyte (working electrode: highly oriented pyrolytic graphite; pseudo reference electrode: Ag^{+/0}; counter electrode: Pt wire). Ferrocene was used as an internal potential reference.

More negative cathodic scans with each bimetallic complex led to further unique electrochemical reductions; these are mostly irreversible and can tentatively be assigned to metal-centered events (see Figures S22-S23). In particular, after the initial quasi-reversible reduction, the isomers of $[\text{Re}(\text{CO})_3\text{Cl}]_2(\text{bpm})$ undergo a further quasi-reversible reduction at -1.46 V followed by an irreversible reduction at -2.37 V. CVs of the homobimetallic Mn species are more complex; the mixture of isomers displayed irreversible reductions at -1.49 V and -2.14 V, as well as several oxidations, suggesting that there are coupled chemical reactions that result in formation of multiple new species. For the mixture of syn and anti isomers of $[\text{Re}(\text{CO})_3\text{Br}(\text{bpm})\text{Mn}(\text{CO})_3\text{Br}]$, three additional irreversible reductions are observed at -1.40 V, -1.93 V, and -2.27 V, as well as several oxidations, implying that this complex also undergoes reduction-induced chemical reactivity, the products of which have not been investigated here. However, the value of the comproportionation constant K_c for the singly reduced, paramagnetic intermediate (*vide infra*) can be computed for $[\text{Re}(\text{CO})_3\text{Cl}]_2(\text{bpm})$ based upon the difference between the first and second reduction potentials.⁶¹ This value is estimated to be $10^{10.8}$, a high value consistent with the large separation (640 mV) between the first and second reductions of $[\text{Re}(\text{CO})_3\text{Cl}]_2(\text{bpm})$ that indicates strong coupling between the redox-active centers here.

Electron paramagnetic resonance studies

Based on the electrochemical profile of the mixture of syn and anti isomers of $[\text{Re}(\text{CO})_3\text{Cl}]_2(\text{bpm})$, we next set out to study the chemical reduction of these complexes in order to provide evidence for the assignment of the initial reductions as either

ligand- or metal-based. Specifically, we targeted the 1e⁻ chemical reduction of the mixture of syn and anti isomers of $[\text{Re}(\text{CO})_3\text{Cl}]_2(\text{bpm})$ to complement previously reported spectroelectrochemical (SE) electron paramagnetic resonance (EPR) results of **1** and $[\text{Re}(\text{CO})_3\text{Cl}]_2(\text{bpm})$.^{39,49,50,62} In an *in situ* reduction experiment, treatment of the mixture of syn and anti isomers of $[\text{Re}(\text{CO})_3\text{Cl}]_2(\text{bpm})$ with 1.0 equiv. of cobaltocene (Cp_2Co , $E_{1/2} = -1.34$ V vs. $\text{Fc}^{+/0}$)⁶³ in CD_3CN resulted in a rapid color change; analysis by ¹H NMR revealed the presence of cobaltocenium ($[\text{Cp}_2\text{Co}]^+$ at 5.66 ppm, see Figures S8 and S32) as the primary diamagnetic product.⁶⁴ Simultaneously, the disappearance of the signals associated with the mixture of syn and anti isomers of $[\text{Re}(\text{CO})_3\text{Cl}]_2(\text{bpm})$ confirmed conversion of the diamagnetic starting materials into paramagnetic products. Although these products could not be isolated cleanly due to similar solubility profiles with $[\text{Cp}_2\text{Co}]^+$, EPR was used to interrogate the mixture further. For the EPR analysis, the syn and anti isomers of $[\text{Re}(\text{CO})_3\text{Cl}]_2(\text{bpm})$ were dissolved in toluene, frozen in a quartz EPR tube held at 78 K, and an equimolar solution of Cp_2Co was layered on top; the entire sample was then refrozen. The air-sensitive sample was then brought out of the glovebox, frozen in liquid nitrogen, and transported to the EPR spectrometer. When the sample was ready for measurement, it was briefly thawed to allow the two layers to mix and then quickly refrozen before interrogation by EPR spectroscopy.

EPR data for the sample revealed an isotropic signal at $g = 2$ (see Figure 4), consistent with formation of a bpm ligand-centered radical. This result mirrors findings from the prior work based upon spectroelectrochemical methods carried out by Kaim and Kohlmann.³⁹ Our experimental data was modelled using the Easyspin⁶⁵ package in MATLAB; a satisfactory match between the experimental data and the simulated data was obtained with a single-component system centered at $g = 1.999$, consistent with the expected similarity of the singly reduced forms of the syn and anti isomers of $[\text{Re}(\text{CO})_3\text{Cl}]_2(\text{bpm})$. Thus, the EPR signal observed upon the first electrochemical reduction can be assigned to a ligand-centered radical. Based on the similar voltammetric properties among all the bimetallic species, we anticipate that the first reductions of $[\text{Mn}(\text{CO})_3\text{Br}]_2(\text{bpm})$ and $[\text{Re}(\text{CO})_3\text{Br}(\text{bpm})\text{Mn}(\text{CO})_3\text{Br}]$ are also ligand centered.

3. Conclusions

The novel bimetallic complexes $[\text{Mn}(\text{CO})_3\text{Br}]_2(\text{bpm})$ and $[\text{Re}(\text{CO})_3\text{Br}(\text{bpm})\text{Mn}(\text{CO})_3\text{Br}]$ were synthesized as an inseparable mixture of syn and anti isomers in solution; the compounds displayed characteristic spectra that confirm their expected symmetry characteristics. The solid-state structures of **1**, **2-anti**, **3**, **4**, **5-syn**, **5-anti**, and **6-syn** provided data for comparison of metrical parameters that differentiate the monometallic and bimetallic complexes. In particular, the data suggest that an inductive effect arises from incorporation of an additional tricarbonyl unit in the bimetallic compounds. The inductive effect was confirmed using cyclic voltammetry; shifts of greater than 380 mV were measured for the initial reductions

of the bimetallic species in comparison to their monometallic analogues. Experimental EPR data and simulations for one derivative suggest that these initial reductions are ligand centered. Taken together, these studies confirm that 2,2'-bipyrimidine is a useful ligand for formation of modular bimetallic metal tricarbonyl complexes.

4. Experimental Section

General considerations

All manipulations were carried out in dry N₂-filled gloveboxes (Vacuum Atmospheres Co., Hawthorne, CA, USA) or under an N₂ atmosphere using standard Schlenk techniques unless otherwise noted. All solvents were of commercial grade and dried over activated alumina using a PPT Glass Contour (Nashua, NH, USA) solvent purification system prior to use, and were stored over molecular sieves. All chemicals were obtained from major commercial suppliers. Manganese pentacarbonyl bromide (98%, Strem Chemical Co.) rhenium pentacarbonyl bromide (98%, Strem Chemical Co.), rhenium pentacarbonyl chloride (98%, Strem Chemical Co.), 2,2'-bipyrimidine (95%, Sigma Aldrich), and 2,2'-bipyrazine (97%, TCI Chemicals) were used as received. Re(CO)₅Cl(bpm),³⁶ [Re(CO)₅Cl]₂(bpm),³⁶ Mn(CO)₅Br(bpz),²³ and Mn(CO)₅Br(bpm)⁴² were prepared according to previously reported literature procedures. Deuterated solvents for NMR studies were purchased from Cambridge Isotope Laboratories (Tewksbury, MA, USA); CD₃CN was dried and stored over 3 Å molecular sieves.

¹H NMR spectra were collected on 400 MHz Bruker spectrometers (Bruker, Billerica, MA, USA) and referenced to the residual protio-solvent signal. Infrared spectra were collected on a PerkinElmer Spectrum 100 Fourier transform infrared spectrometer. Electronic absorption spectra were collected with an Ocean Optics Flame spectrometer equipped with a DH-Mini light source (Ocean Optics, Largo, FL, USA) using a quartz cuvette. Experimental high resolution mass spectrometry data were collected on a LCT Premier mass spectrometer equipped with a quadrupole, time-of-flight mass analyzer, and an electrospray ion source, or with a PE SCIEX API 365 triple quadrupole spectrometer. Predicted mass spectrometry data were obtained from PerkinElmer Informatics' ChemDraw Professional Suite. Continuous-wave electron paramagnetic resonance spectra were collected at X-band with a Bruker EMX spectrometer using a high-sensitivity perpendicular-mode cavity (4119HS-W1). Temperature control was achieved with an Oxford ESR 900 flow-through cryostat. Elemental analyses were performed by Midwest Microlab, Inc. (Indianapolis, IN, USA).

X-Ray diffraction procedures

Crystals were mounted on polyimide MiTeGen loops with STP Oil Treatment and placed under a nitrogen stream. Low temperature (100 K) X-ray data were collected on a Bruker AXS D8 KAPPA diffractometer with an APEX II CCD detector and TRIUMPH graphite monochromator running at 50 kV and 30 mA

with Mo radiation ($K_{\alpha} = 0.71073 \text{ \AA}$) for **1** and on a Bruker AXS D8 VENTURE KAPPA diffractometer with PHOTON 100 CMOS detector and Helios focusing multilayer mirror optics running at 50 kV and 1 mA using Cu radiation ($K_{\alpha} = 1.54178 \text{ \AA}$) for **5-syn** and **5-anti** and using Mo radiation ($K_{\alpha} = 0.71073 \text{ \AA}$) for **2-anti**, **3**, **4**, and **6-syn**. Totals of 2374 (**1**), 2053 (**2-anti**), 2444 (**3**), 1206 (**4**), 1338 (**5-syn**), 2013 (**5-anti**), 884 (**6-syn**), 0.5° or 1.0°-wide ω - or ϕ -scan frames were collected with counting times of 10-20 seconds (**1**), 4-30 seconds (**2**), 1-10 seconds (**3**), 1-20 seconds (**4**), 5-60 seconds (**5-syn**), 1-15 seconds (**5-anti**), and 2-60 seconds (**6-syn**). Preliminary lattice constants were obtained with the Bruker Apex2 Software Suite.⁶⁶ Integrated reflection intensities for all compounds were produced using SAINT in the Bruker Apex2 Software Suite. Each data set was corrected empirically for variable absorption effects with SADABS⁶⁷ using equivalent reflections. The Bruker software package SHELXTL was used to solve each structure using intrinsic direct methods phasing. Final stages of weighted full-matrix least-squares refinement were conducted using F_o² data with SHELXTL⁶⁸ or the Olex2 software package equipped with XL⁶⁹. All non-hydrogen atoms were refined anisotropically. All hydrogen atoms were included into the model at geometrically calculated positions and refined using a riding model. The isotropic displacement parameters of all hydrogen atoms were fixed to 1.2 times the *U* value of the atoms they are linked to. The relevant crystallographic and structure refinement data for all seven structures are given in Table S1.

Electrochemistry

Electrochemical experiments were carried out in a nitrogen-filled glove box (in the dark for Mn-containing samples). 0.10 M tetra(n-butylammonium) hexafluorophosphate (Sigma-Aldrich; electrochemical grade) in acetonitrile served as the supporting electrolyte. Measurements were made with a Gamry Reference 600 Plus Potentiostat/ Galvanostat using a standard three-electrode configuration. The working electrode was the basal plane of highly oriented pyrolytic graphite (HOPG, GraphiteStore.com, Buffalo Grove, Ill.; surface area: 0.09 cm²), the counter electrode was a platinum wire (Kurt J. Lesker, Jefferson Hills, PA; 99.99%, 0.5 mm diameter), and a silver wire immersed in electrolyte served as a pseudo-reference electrode (CH Instruments). The reference was separated from the working solution by a Vycor frit (Bioanalytical Systems, Inc.). Ferrocene (Sigma Aldrich; twice-sublimed) was added to the electrolyte solution at the conclusion of each experiment (~1 mM); the midpoint potential of the ferrocenium/ferrocene couple (denoted as Fc⁺⁰) served as an external standard for comparison of the recorded potentials. Concentrations of analyte for cyclic voltammetry were typically 1 mM.

Synthetic procedures

Synthesis of [Mn(CO)₅Br]₂(bpm)] (5). In the dark, 2,2'-bipyrimidine (0.0996 g, 0.630 mmol) was dissolved in toluene (35 mL). Mn(CO)₅Br was added (0.3563 g, 1.30 mmol) and the solution refluxed under N₂ for 4 hours. The solution was then allowed to cool, the precipitate collected by vacuum filtration, and washed with diethyl ether. The pure solid was then dried

under vacuum before storing in the dark (0.3408 g, 91% yield). ^1H NMR (400 MHz, CD_3CN) δ 9.43 (d, $^3J_{\text{H,H}} = 5.5$ Hz, 4H), 7.85 (t, $^3J_{\text{H,H}} = 5.5$ Hz, 2H). Resolved isomer: δ 9.46 (d, $^3J_{\text{H,H}} = 5.5$ Hz, 4H), 7.88 (t, $^3J_{\text{H,H}} = 5.5$ Hz, 2H). A comparison of the resolved doublet peaks near δ 9.45 ppm revealed that the desired product was present in two isomeric forms in the ratio 3.14 to 1. High Resolution ESI-MS (positive) m/z : expected 555.8497; found 555.8495 (**5** – Br^- + NCMe). Electronic absorption spectrum (MeCN): 250 (4200), 369 (1600), 510 nm ($750 \text{ M}^{-1} \text{ cm}^{-1}$). IR (THF): $\nu_{\text{C=O}}$ 2031 (m), $\nu_{\text{C=O}}$ 1952 (m), and $\nu_{\text{C=O}}$ 1936 (m) cm^{-1} . Anal. Calcd. for $\text{Mn}_2\text{C}_{14}\text{H}_6\text{Br}_2\text{N}_4\text{O}_6$: C, 28.22; H, 1.01; N, 9.40. Found: C, 28.00; H, 1.11; N, 9.21.

Synthesis of $[\text{Re}(\text{CO})_3\text{Br}(\text{bpm})\text{Mn}(\text{CO})_3\text{Br}]$ (6**).** 2,2'-bipyrimidine (0.1516 g, 0.959 mmol) was dissolved in toluene (35 mL). $\text{Re}(\text{CO})_5\text{Br}$ was added (0.3478 g, 0.856 mmol) and the solution refluxed under N_2 for 22 hours. The solution was then allowed to cool and the resulting precipitate collected by vacuum filtration and washed with diethyl ether. The pure solid was then dried under vacuum. In the absence of light, a portion of pure product (0.0996 g, 0.245 mmol) was dissolved in toluene (35 mL). Then $\text{Mn}(\text{CO})_5\text{Br}$ was added (0.0557 g, 0.203 mmol) and the solution refluxed under N_2 for 12 hours. The solution was then allowed to cool and the resulting precipitate collected by vacuum filtration and washed with diethyl ether. The pure solid was then dried under vacuum before storing in the dark (0.1313g, 89% yield). ^1H NMR (400 MHz, CD_3CN) δ 9.52 (dd, $^3J_{\text{H,H}} = 5.6$ Hz, $^4J_{\text{H,H}} = 1.7$ Hz, 2H), 9.27 (dd, $^3J_{\text{H,H}} = 5.6$ Hz, $^4J_{\text{H,H}} = 1.7$ Hz, 2H), 7.86 (t, $^3J_{\text{H,H}} = 5.6$ Hz, 2H) ppm. Resolved isomer: δ 9.55 (dd, $^3J_{\text{H,H}} = 5.6$ Hz, $^4J_{\text{H,H}} = 1.7$ Hz, 2H), 9.30 (dd, $^3J_{\text{H,H}} = 5.6$ Hz, $^4J_{\text{H,H}} = 1.7$ Hz, 2H), 7.89 (t, $^3J_{\text{H,H}} = 5.6$ Hz, 2H) ppm. A comparison of the resolved doublet peaks near δ 9.54 ppm revealed that the desired product was present in two isomeric forms in the ratio 1.80 to 1. High Resolution ESI-MS (positive) m/z : expected: 687.8674; found: 687.8672 (**6** – Br^- + NCMe). Electronic absorption spectrum (MeCN): 243 (28000); 365 (5800); 515 nm ($2200 \text{ M}^{-1} \text{ cm}^{-1}$). IR (THF): $\nu_{\text{C=O}}$ 2028 (m), $\nu_{\text{C=O}}$ 1951 (m), and $\nu_{\text{C=O}}$ 1935 (m), 1914 (m) cm^{-1} . Anal. Calcd. for $\text{MnReC}_{14}\text{H}_6\text{Br}_2\text{N}_4\text{O}_6$: C, 23.12; H, 0.83; N, 7.70. Found: C, 23.14; H, 0.85; N, 7.61.

¹ (a) D. J. Stufkens and A. Vlcek, *Coord. Chem. Rev.*, 1998, **177**, 127-179. (b) A. El Nahhas, C. Consani, A. M. Blanco-Rodriguez, K. M. Lancaster, O. Braem, A. Cannizzo, M. Towrie, I. P. Clark, S. Zalis, M. Chergui and A. Vlcek, *Inorg. Chem.*, 2011, **50**, 2932-2943.

² (a) L. Wallace and D. P. Rillema, *Inorg. Chem.*, 1993, **32**, 3836-3843. (b) R. J. Shaver, M. W. Perkovic, D. P. Rillema and C. Woods, *Inorg. Chem.*, 1995, **34**, 5446-5454.

³ A. Léval, H. Junge, and M. Beller, *Catal. Sci.*, 2020, **10**, 3931-3937.

⁴ (a) U. Schatzschneider, *Inorg. Chim. Acta*, 2011, **374**, 19-23. (b) R. Alberto, R. Schibli, A. Egli, A. P. Schubiger, U. Abram, and T. A. Kaden, *J. Am. Chem. Soc.*, 1998, **120**, 7987-7988.

⁵ M. N. Pinto, I. Chakraborty, C. Sandoval and P. K. Mascharak, *J. Controlled Release*, 2017, **264**, 192-202.

⁶ (a) J. Hawecker, J. M. Lehn and R. Ziessel, *J. Chem. Soc.*,

Conflicts of interest

There are no conflicts to declare.

Acknowledgements

The authors thank Dr. Justin Douglas and Sarah Neuenswander for assistance with NMR and EPR spectroscopy. This work was supported by the U.S. National Science Foundation through awards OIA-1833087 and CHE-1305124. W.C.H. was supported by the U.S. National Institutes of Health Graduate Training Program in the Dynamic Aspects of Chemical Biology (T32 GM008545-25).

The authors also acknowledge the U.S. National Science Foundation and U.S. National Institutes of Health for support of the EPR instrumentation (CHE-0946883) and NMR instrumentation (S10OD016360, S10RR024664, and CHE-0320648) used in this study. The Bruker D8 Kappa X-ray diffractometer used for **1** was purchased via an NSF CRIF:MU award to the California Institute of Technology (CHE-0639094). A Dow Next Generation Instrumentation Grant supported the work on **2-anti**, **3**, **4**, **5-syn**, **5-anti**, and **6-syn**.

Notes and References

† Current Address: Department of Chemistry, University of California at Irvine, Irvine, California 92617, USA.

‡ Current Address: Department of Chemistry, Northwestern University, Evanston, Illinois 60208, USA.

References

- Chem. Commun.*, 1984, 328-330. (b) B. P. Sullivan, C. M. Bolinger, D. Conrad, W. J. Vining, T. J. Meyer, *J. Chem. Soc. Chem. Commun.*, 1985, 1414-1416.
- ⁷ M. Bourrez, F. Molton, S. Chardon-Noblat, and A. Deronzier, *Angew. Chem. Int. Ed.*, 2011, **50**, 9903-9906.
- ⁸ J. C. Luong, R. A. Faltynek, and M. S. Wrighton, *J. Am. Chem. Soc.*, 1980, **102**, 7892-7900.
- ⁹ J. V. Caspar and T. J. Meyer, *J. Phys. Chem.*, 1983, **87**, 952-957.
- ¹⁰ D. Miguel and V. Riera, *J. Organomet. Chem.*, 1985, **293**, 379-390.
- ¹¹ H. Takeda, K. Koike, H. Inoue, and O. Ishitani, *J. Am. Chem. Soc.*, 2008, **130**, 2023-2031.
- ¹² J.M. Smieja and C.P. Kubiak, *Inorg. Chem.*, 2010, **49**, 9283-9289.

- ¹³ B. Gholamkhash, H. Mametsuka, K. Koike, T. Tanabe M. Furue and O. Ishitani, *Inorg. Chem.*, 2005, **44**, 2326-2336.
- ¹⁴ P. Kurz, B. Probst, B. Spingler, and R. Alberto, *Eur. J. Inorg. Chem.*, 2006, **2006**, 2966-2974.
- ¹⁵ J. Etedgui, Y. Diskin-Posner, L. Weiner, and R. Neumann, *J. Am. Chem. Soc.*, 2011, **133**, 188-190.
- ¹⁶ J. M. Smieja, M. D. Sampson, K. A. Grice, E. E. Benson, J. D. Froehlich, and C. P. Kubiak, *Inorg. Chem.*, 2013, **52**, 2484-2491.
- ¹⁷ H. Fei, M. D. Sampson, Y. Lee, C. P. Kubiak, and S. M. Cohen, *Inorg. Chem.*, 2015, **54**, 6821-6828.
- ¹⁸ K. T. Ngo, M. McKinnon, B. Mahanti, R. Narayanan, D. C. Grills, M. Z. Ertem, and J. Rochford, *J. Am. Chem. Soc.*, 2017, **139**, 2604-2618.
- ¹⁹ J. Agarwal, T. W. Shaw, H. F. Schaefer, and A. B. Bocarsly, *Inorg. Chem.*, 2015, **54**, 5285-5294.
- ²⁰ (a) K. J. Kadassery, S. N. MacMillan, and D. C. Lacy, *Dalton Trans.*, 2018, **47**, 12652-12655. (b) K. J. Kadassery and D. C. Lacy, *Dalton Trans.*, 2019, **48**, 4467-4470.
- ²¹ W. C. Henke, C. J. Otolski, W. N. G. Moore, C. G. Elles, and J. D. Blakemore, *Inorg. Chem.* 2020, **59**, 2178-2187.
- ²² M. L. Clark, P. L. Cheung, M. Lessio, E. A. Carter, and C. P. Kubiak, *ACS Catal.*, 2018, **8**, 2021-2029.
- ²³ S. E. Tignor, H.-Y. Kuo, T. S. Lee, G. D. Scholes, and A. B. Bocarsly, *Organometallics*, 2019, **38**, 1292-1299.
- ²⁴ W.C. Henke, J.A. Hopkins, M.L. Anderson, J.P. Stiel, V.W. Day, and J.D. Blakemore, *Molecules*, 2020, **25**, 3189-3203.
- ²⁵ (a) J. S. Kanady, E. Y. Tsui, M. W. Day, T. Agapie, *Science*, 2011, **333**, 733-736. (b) E. Y. Tsui, R. Tran, J. Yano, T. Agapie, *Nat. Chem.*, 2013, **5**, 293-299.
- ²⁶ J. P. Krogman, B. M. Foxman and C. M. Thomas, *J. Am. Chem. Soc.*, 2011, **133**, 14582-14585.
- ²⁷ A. H. Reath, J. W. Ziller, C. Tsay, A. J. Ryan, J.Y. Yang, *Inorg. Chem.*, 2017, **56**, 3713-3718.
- ²⁸ A. Kumar, D. Lionetti, V. W. Day, and J. D. Blakemore, *Chem. Eur. J.*, 2018, **24**, 141-149.
- ²⁹ P. Sharma, D. R. Pahls, B. L. Ramirez, C. C. Lu and L. Gagliardi, *Inorg. Chem.* 2019, **58**, 10139-10147.
- ³⁰ A. Kumar, D. Lionetti, V. W. Day, and J. D. Blakemore, *J. Am. Chem. Soc.*, 2020, **142**, 3032-3041.
- ³¹ Y. Tamaki, D. Imori, T. Morimoto, K. Koike, and O. Ishitani, *Dalton Trans.*, 2016, **45**, 14668-14677.
- ³² D.A. Popov, J.M. Luna, N.M. Orchanian, R. Haiges, C.A. Downes, S.C. Marinescu, *Dalton Trans.*, 2018, **47**, 17450-17460.
- ³³ (a) W. Yang, S. Sinha Roy, W. C. Pitts, R. L. Nelson, F. R. Fronczek and J. W. Jurss, *Inorg. Chem.*, 2018, **57**, 9564-9575. (b) N. P. Liyanage, W. Yang, S. Guertin, S. S. Roy, C. A. Carpenter, R. E. Adams, R. H. Schmehl, J. H. Delcamp, and J. W. Jurss, *Chem. Commun.*, 2019, **55**, 993-996.
- ³⁴ (a) M. Hunziker and A. Ludi, *J. Am. Chem. Soc.*, 1977, **99**, 7370-7371. (b) R. R. Ruminski and J. D. Petersen, *Inorg. Chem.*, 1982, **21**, 3706-3708. (c) K. J. Brewer, W. R. Murphy and J. D. Petersen, *Inorg. Chem.*, 1987, **26**, 3376-3379. (d) W. Kaim, A. Klein and M. Glöckle, *Acc. Chem. Res.*, 2000, **33**, 755-763.
- ³⁵ J. J. Concepcion, J. W. Jurss, P. G. Hoertz, T. J. Meyer, *Angew. Chem. Int. Ed.*, 2009, **48**, 9473-9476.
- ³⁶ A. Vogler, and J. Kisslinger, *Inorganica Chim. Acta*, 1986, **115**, 193-196.
- ³⁷ K. D. Benkstein, J. T. Hupp, and C. L. Stern, *J. Am. Chem. Soc.*, 1998, **120**, 12982-12983.
- ³⁸ A. Juris, S. Campagna, I. Bidd, J. M. Lehn and R. Ziessel, *Inorg. Chem.*, 1988, **27**, 4007-4011.
- ³⁹ (a) W. Kaim and S. Kohlmann, *Chem. Phys. Lett.*, 1987, **139**, 365-369. (b) W. Kaim and S. Kohlmann, *Inorg. Chem.*, 1990, **29**, 2909-2914.
- ⁴⁰ K. Pollborn, B. Aechter, and W. Beck, *Z. Kristallogr. – New Cryst. Struct.*, 2001, **216**, 407-408.
- ⁴¹ Syn and anti is the preferred IUPAC nomenclature for the isomers of the compounds. IUPAC. Compendium of Chemical Terminology, 2nd ed. (the "Gold Book"). Compiled by A. D. McNaught and A. Wilkinson. Blackwell Scientific Publications, Oxford (1997). Online version (2019-) created by S. J. Chalk. ISBN 0-9678550-9-8. <https://doi.org/10.1351/goldbook>
- ⁴² P. Kumar, C. Joshi, A. K. Srivastava, P. Gupta, R. Boukherroub, and S. L. Jain, *ACS Sustain. Chem. Eng.*, 2016, **4**, 69-75.
- ⁴³ J. W. M. van Outersterp, D. J. Stufkens, J. Fraanje, K. Goubitz, and A. Vlcek, *Inorg. Chem.*, 1995, **34**, 4756-4766.
- ⁴⁴ K. Polborn, B. Aechter, W. Beck, *Z. Kristallog.-New Cryst. Struct.*, 2001, **216**, 407-408.
- ⁴⁵ N. M. Shavaleev, Z. R. Bell, and M. D. Ward, *J. Chem. Soc., Dalton Trans.*, 2002, 3925-3927.
- ⁴⁶ N. M. Shavaleev, G. Accorsi, D. Virgili, Z. R. Bell, T. Lazarides, G. Calogero, N. Armaroli, and M. D. Ward, *Inorg. Chem.*, 2005, **44**, 61-72.
- ⁴⁷ B. Aechter, J. Knizek, H. Noth, W. Beck, *Z. Kristallog.-New Cryst. Struct.*, 2005, **220**, 110.
- ⁴⁸ H. Takeda, H. Koizumi, K. Okamoto, and O. Ishitani, *Chem. Commun.*, 2014, **50**, 1491-1493.
- ⁴⁹ A. Klein, C. Vogler, and W. Kaim, *Organometallics*, 1996, **15**, 236-244.
- ⁵⁰ W. Kaim, T. Scheiring, M. Weber, J. Fiedler, *Z. Anorg. Allg. Chem.*, 2004, **630**, 1883-1893.
- ⁵¹ T. J. Meyer, *Pure Appl. Chem.*, 1986, **58**, 1193-1206.
- ⁵² R. Heydová, E. Gindensperger, R. Romano, J. Sýkora, A. Vlček, S. Zálaiš and C. Daniel, *J. Phys. Chem. A*, 2012, **116**, 11319-11329.
- ⁵³ C. R. Groom, I. J. Bruno, M. P. Lightfoot, S. C. Ward, The Cambridge Structural Database. *Acta Cryst. Sec. B*, 2016, **72**, 171-179.
- ⁵⁴ P. Kurz, B. Probst, B. Spingler, and R. Alberto, *Eur. J. Inorg. Chem.*, 2006, **15**, 2966-2974.
- ⁵⁵ R. Kia and F. Safari, *Inorg. Chim. Acta*, 2016, **453**, 357-368.
- ⁵⁶ I. Chakraborty, S. J. Carrington, and P. K. Mascharak, *ChemMedChem*, 2014, **9**, 1266-1274.
- ⁵⁷ L. Fernoholt, C. Rømming, and S. Samdal, *Acta. Chem. Scand.* 1981, **35a**, 707-715.
- ⁵⁸ (a) J. J. Soldevila-Barreda, A. Habtemariam, I. Romero-Canelón, and P.J. Sadler, *J. Inorg. Biochem.*, 2015, **153**, 322-333. (b) J.D. Blakemore, E.S. Hernandez, W. Sattler, B.M. Hunter, L.M. Henling, B.S. Brunshwig, H.B. Gray, *Polyhedron*, 2014, **84**, 14-18.
- ⁵⁹ C. Creutz, *Comments Inorg. Chem.*, 1982, **1**, 293-311.

- ⁶⁰ F. Hartl, B. D. Rossenaar, G. J. Stor and D. J. Stufkens, *Recl. Trav. Chim. Pays-Bas*, 1995, **114**, 565-570.
- ⁶¹ (a) H. Hartmann, W. Kaim, M. Wanner, A. Klein, S. Frantz, C. Duboc-Toia, J. Fiedler and S. Zális, *Inorg. Chem.*, 2003, **42**, 7018-7025. (b) P. J. Ball, T. R. Shtoyko, J. A. Krause Bauer, W. J. Oldham and W. B. Connick, *Inorg. Chem.*, 2004, **43**, 622-632.
- ⁶² W. Kaim, H. E. A. Kramer, C. Vogler, and J. Rieker, *J. Organomet. Chem.* 1989, **367**, 107-115.
- ⁶³ N. G. Connelly and W. E. Geiger, *Chem. Rev.*, 1996, **96**, 877-910.
- ⁶⁴ S. Vanicek, H. Kopacka, K. Wurst, T. Müller, H. Schottenberger and B. Bildstein, *Organometallics*, 2014, **33**, 1152–1156.
- ⁶⁵ S. Stoll and A. Schweiger, *J. Magn. Res.*, 2006, **178**, 42-55.
- ⁶⁶ APEX2, Version 2 User Manual, M86-E01078,; Bruker Analytical X-ray Systems: Madison, WI, June 2006.
- ⁶⁷ G. M. Sheldrick, SADABS (version 2008/1): Program for Absorption Correction for Data from Area Detector Frames, University of Göttingen, 2008.
- ⁶⁸ G. M. Sheldrick, Crystal structure refinement with SHELXL. *Acta Crystallogr., Sect. A: Found. Crystallogr.* 2015, **71**, 3-8.
- ⁶⁹ O. V. Dolomanov, L. J. Bourhis, R. J. Gildea, J. A. K. Howard, H. J. Puschmann, *Appl. Crystallogr.* 2009, **42**, 339-341.